

Targeting of the Cystic Fibrosis Transmembrane Conductance Regulator (CFTR) Protein with a Technetium-99m Imaging Probe

Vera F. C. Ferreira,^[a] Bruno L. Oliveira,^[a, c] João D. Santos,^[b] João D. G. Correia,^[a] Carlos M. Farinha,^[b] and Filipa Mendes^{*[a]}

Cystic fibrosis (CF) is caused by mutations in the gene that encodes the CF transmembrane conductance regulator (CFTR) protein. The most common mutation, F508del, leads to almost total absence of CFTR at the plasma membrane, a defect potentially corrected via drug-based therapies. Herein, we report the first proof-of-principle study of a noninvasive imaging probe able to detect CFTR at the plasma membrane. We radio-labeled the CFTR inhibitor, CFTR_{inh}-172a, with technetium-99m via a pyrazolyl-diamine chelating unit, yielding a novel

^{99m}Tc(CO)₃ complex. A non-radioactive surrogate showed that the structural modifications introduced in the inhibitor did not affect its activity. The radioactive complex was able to detect plasma membrane CFTR, shown by its significantly higher uptake in wild-type versus mutated cells. Furthermore, assessment of F508del CFTR pharmacological correction in human cells using the radioactive complex revealed differences in corrector versus control uptake, recapitulating the biochemical correction observed for the protein.

Introduction

Cystic fibrosis (CF) is the most common autosomal recessive disorder in Caucasians. Clinically, CF is characterized by a progressive loss of lung function associated with recurrent respiratory infections—the major cause of mortality and morbidity—but also by pancreatic insufficiency, increased chloride concentration in the sweat, and infertility (in males). CF is caused by mutations in the gene that encodes the CF transmembrane conductance regulator (CFTR) protein.^[1] CFTR functions as a chloride channel at the apical surface of epithelia, serving as a major regulator of overall ion and fluid transport. From the more than 2000 CF mutations described, the deletion of a phenylalanine residue at position 508 in the polypeptide chain (F508del) is the most common mutation, present in more than 85% of patients in at least one allele. The F508del mutation impairs CFTR protein folding, leading to its premature degradation and therefore, to almost complete absence of protein at the apical plasma membrane (PM).^[2]

Importantly, F508del CFTR can be rescued to the PM by incubation at low temperature or with the help of chaperones,^[3]

and once there, temperature-corrected F508del CFTR exhibits a shortened half-life^[4] and a major gating defect as an ion channel.^[5] In recent years, small molecules that correct CFTR trafficking have emerged mainly due to the development of high-throughput screening. VX-809, also called lumacaftor, is one of the correctors for F508del CFTR identified so far.^[6] In a phase IIa clinical study, a significant improvement in sweat chloride levels of adult patients with two copies of the F508del mutation suggested that F508del CFTR correction was possible in CF patients.^[7] However, lumacaftor did not present therapeutic benefit in lung function, suggesting the need of a combined therapy of CFTR correctors and potentiators to enhance the function of corrector-rescued CFTR. In 2015, the US Food and Drug Administration (FDA) approved the first drug directed at treating the cause of CF in patients with two copies of the F508del mutation, consisting in the combination of lumacaftor with a CFTR potentiator (ivacaftor).^[8] Other clinical trials assessing dual and triple combination treatment regimens are underway.^[9]

Clinically, pharmacological correction of mutant CFTR protein is assessed by the patient outcome in terms of benefit into sweat chloride and nasal potential difference.^[10] In preclinical imaging, the most recent image-based assays for the surface detection of F508del CFTR involve fusing a fluorophore or a fluorogen-activating protein to the N-terminus of F508del CFTR and transfection to non-polarized human cells.^[11] To our knowledge, there is no available methodology to noninvasively image corrector-rescued F508del CFTR in living organisms (model animals or human subjects).

Nuclear molecular imaging might help to address this need. Considering the array of available noninvasive imaging techniques used in the clinical setting, single-photon emission

[a] V. F. C. Ferreira, Dr. B. L. Oliveira, Dr. J. D. G. Correia, Dr. F. Mendes
C²TN—Centro de Ciências e Tecnologias Nucleares, Instituto Superior Técnico, Universidade de Lisboa, Estrada Nacional 10, 2695-066 Bobadela LRS (Portugal)
E-mail: fmendes@ctn.tecnico.ulisboa.pt

[b] J. D. Santos, Prof. Dr. C. M. Farinha
BioISI—Biosystems and Integrative Sciences Institute, Faculty of Sciences, Universidade de Lisboa, Campo Grande C8, 1749-016 Lisboa (Portugal)

[c] Dr. B. L. Oliveira
Current address: Department of Chemistry, University of Cambridge, Lensfield Road, Cambridge (UK)

Supporting information and the ORCID identification number(s) for the author(s) of this article can be found under:
<https://doi.org/10.1002/cmdc.201800187>

computed tomography (SPECT) and positron emission tomography (PET) are the most sensitive. These techniques are used for the diagnosis and follow-up of therapeutic strategies in several diseases, for instance in cancer, and in the fields of cardiology and neurology.^[12] Technetium-99m (^{99m}Tc) is used in more than 90% of all diagnostic SPECT procedures in nuclear medicine due to its short half-life (≈ 6 h), ideal γ -ray energy (140 keV), low cost, and easy availability. One of the most promising and developed organometallic cores for radiolabeling of biomolecules with ^{99m}Tc is the ^{99m}Tc(I)-tricarbonyl core [^{99m}Tc(CO)₃]⁺.^[13] The synthetic precursor [^{99m}Tc(H₂O)₃(CO)₃]⁺ contains three tightly coordinated CO ligands and three labile water molecules. In the radiolabeling, the water molecules can be readily replaced by mono-, bi-, or tridentate chelators, the latter forming ^{99m}Tc(I)-tricarbonyl complexes with the highest in vivo stability.^[14] Furthermore, the [^{99m}Tc(CO)₃]⁺ has proven to be stable at high temperatures and extended reaction times.^[15]

The development of a noninvasive SPECT imaging probe capable of detecting CFTR at the PM of human epithelial cells would be a great advantage. This type of probe would be a tool potentially useful for evaluation of pharmacological correction by allowing imaging of F508del CFTR at the epithelia of patients undergoing clinical trials. This would be particularly relevant in the respiratory tract, as the lung is the main pathophysiological organ in CF. Several studies have been performed with PET and SPECT probes, mainly for assessment of lung inflammation,^[16] clearance,^[17] and aerosol delivery,^[18] proving their applicability to CF patients.

Herein we report the synthesis, radiolabeling, and biological evaluation of a CFTR-targeting biomolecule, CFTR_{inh}-172a (Figure 1). This is a potent and rapid voltage-independent

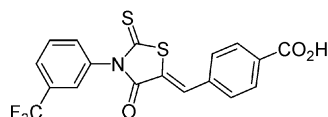


Figure 1. Structure of the CFTR inhibitor CFTR_{inh}-172a.

CFTR inhibitor in human airway cells,^[19] shown to interact specifically with CFTR at the region of the channel pore.^[20] Several inhibitors or antagonists are already being evaluated in clinical PET and SPECT studies as imaging agents for the expression of the prostate-specific membrane antigen in prostate cancers,^[21] the somatostatin receptor in neuroendocrine tumors,^[22] and the chemokine receptor overexpressed in many types of human cancers.^[23] Evidence from preclinical and clinical studies suggest that antagonists or inhibitors may be superior to agonists, and are paving the way to a shift toward such molecules as targeting agents for cancer imaging.^[24]

Our radiolabeling strategy involved a three-component system constituted by the high affinity CFTR-specific targeting unit CFTR_{inh}-172a, a radiometal (^{99m}Tc using the [^{99m}Tc(CO)₃]⁺ core), and a bifunctional chelator (BFC), designed to bind to the radiometal and biomolecule.^[25] In vitro studies were con-

ducted using two cellular models to assess the suitability of the labeled inhibitor as a probe for detecting PM CFTR.

Results and Discussion

Synthesis and radiolabeling of a new CFTR-targeting biomolecule

Knowing that tridentate chelators form stable complexes with the *fac*-[^{99m}Tc(CO)₃]⁺ core,^[14] we first synthesized the BFC precursor **L1-Boc** containing a pyrazolyl-diamine chelating unit (with a *N,N,N* donor atom set), a three-carbon spacer, and a terminal amino group (-NH₂) for conjugation to the carboxyl group present in the CFTR inhibitor CFTR_{inh}-172a.^[13b,26] **L1-Boc** was prepared via a multistep procedure previously reported by our group,^[27] and was characterized by ¹H/¹³C NMR spectroscopy (including 2D NMR experiments such as ¹H-¹H gradient correlation spectroscopy (gCOSY) and ¹H-¹³C gradient heteronuclear single quantum coherence (gHSQC)), and reversed-phase high-performance liquid chromatography (RP-HPLC). CFTR_{inh}-172a was then conjugated to **L1-Boc** using standard coupling conditions, followed by hydrolysis of the protecting group under acidic conditions (Scheme 1, synthetic pathway A). **B1** was obtained as a yellow oil after purification by silica gel chromatography and was characterized by NMR spectroscopy (¹H/¹³C NMR, Figures S1 and S2, Supporting Information, ¹H-¹H gCOSY, and ¹H-¹³C gHSQC), electrospray ionization mass spectrometry (EI-MS), and RP-HPLC. Altogether, the data pointed to the successful synthesis of **B1**.

Synthesis of ^{99m}Tc complexes occurs in very dilute aqueous solutions, making it impossible to characterize these radiocomplexes by the usual analytical techniques in chemistry. Owing to the chemical similarities between Tc and rhenium (Re), the latter has been used to synthesize non-radioactive surrogates of ^{99m}Tc complexes and aid in their structural characterization. Reaction of **B1** with the precursor *fac*-[Re(CO)₃(H₂O)₃]Br afforded **Re1** (Scheme 1, synthetic pathway A) in moderate yield ($\eta = 55\%$).

The novel complex was characterized by ¹H and ¹³C NMR spectroscopy (Supporting Information, Figures S3 and S4), matrix-assisted laser desorption/ionization-time of flight (MALDI/TOF) MS, and RP-HPLC. The tridentate coordination mode of the pyrazolyl-diamine chelating unit to the metal was confirmed by NMR (Supporting Information, Figure S3). We observed a diastereotopic pattern for the protons belonging to this unit, which suggest coordination to the metal, as observed for other Re^I-tricarbonyl complexes synthesized by our group.^[28] ¹³C NMR of **Re1** revealed the presence of three resonances assigned to the CO ligands coordinated to Re.

We confirmed **Re1** synthesis through MALDI/TOF-MS (*m/z* 901.1 [*M*]⁺ (calcd for C₃₃H₃₃F₃N₆O₅ReS₂: 901.2)). Nevertheless, the presence of unassigned species in MS and HPLC analyses and the moderate reaction yield led us to hypothesize that degradation products could be produced during **Re1** synthesis in water at reflux. Because we had previous evidence from our research group that **L1-Boc** would be stable at high temperatures (up to 100 °C),^[27b] we hypothesized that these results

could be associated with the instability of the CFTR_{inh}-172a moiety at high temperatures. Stability analysis of CFTR_{inh}-172a at 100 °C by RP-HPLC showed degradation over time (data not shown). These results indicated that high temperatures would probably affect the inhibitory moiety in **B1**, and consequently, impair the formation of Re^{I/99m}Tc(I)-tricarbonyl complexes.

Aimed at avoiding submission of the inhibitor to high temperatures, an alternative synthetic strategy for **Re1** was adopted (Scheme 1, synthetic pathway B). Firstly, the protecting group of **L1-Boc** was removed under acidic conditions, affording **L1**, which reacted with the *fac*-[Re(CO)₃(H₂O)₃]Br precursor in water at reflux for 16 h. The resulting Re complex **RePz(CH₂)₃NH₂** was purified by RP-HPLC and characterized by EI-MS and ¹H/¹³C NMR spectroscopy (Supporting Information, Figures S5 and S6). **RePz(CH₂)₃NH₂** was then conjugated to CFTR_{inh}-172a using standard coupling conditions at room temperature. After purification by solid-phase extraction using a Sep-Pak C₁₈® cartridge, **Re1** was obtained as a yellow solid and characterized by ¹H NMR spectroscopy (Supporting Information, Figure S7), EI-MS, and RP-HPLC. Data confirmed the presence of **Re1** and absence of the degradation products obtained on synthesis of **Re1** via pathway A.

Bearing in mind the temperature sensitivity of the inhibitory moiety of **B1**, radiolabeling was achieved by reacting it with the organometallic precursor *fac*-[^{99m}Tc(CO)₃(H₂O)₃]⁺ at 50 °C for 30 min. The reaction afforded the radiocomplex *fac*-[^{99m}Tc(CO)₃(κ³-**B1**)], **Tc1**, with high radiochemical purity after RP-HPLC purification (≥ 95%; Figure 2, *t* = 0 h).

The chemical identity of **Tc1** was confirmed by comparing its chromatographic profile (γ-detection) with its non-radioactive surrogate **Re1** (UV/Vis detection). Stability of **Tc1** was tested in biologically relevant solutions as fresh human serum (Figure 2, *t* = 1 h) and cell medium, and the radioactive com-

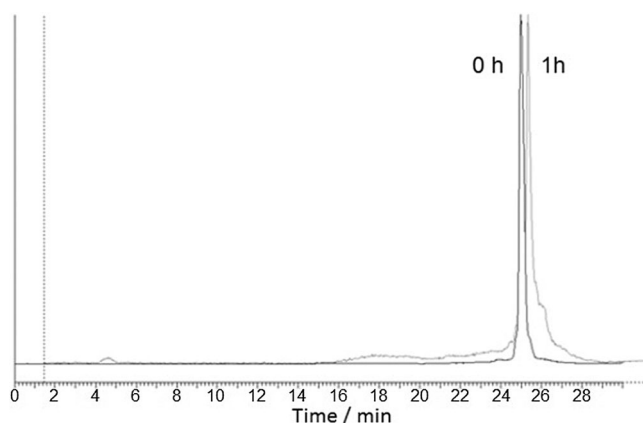


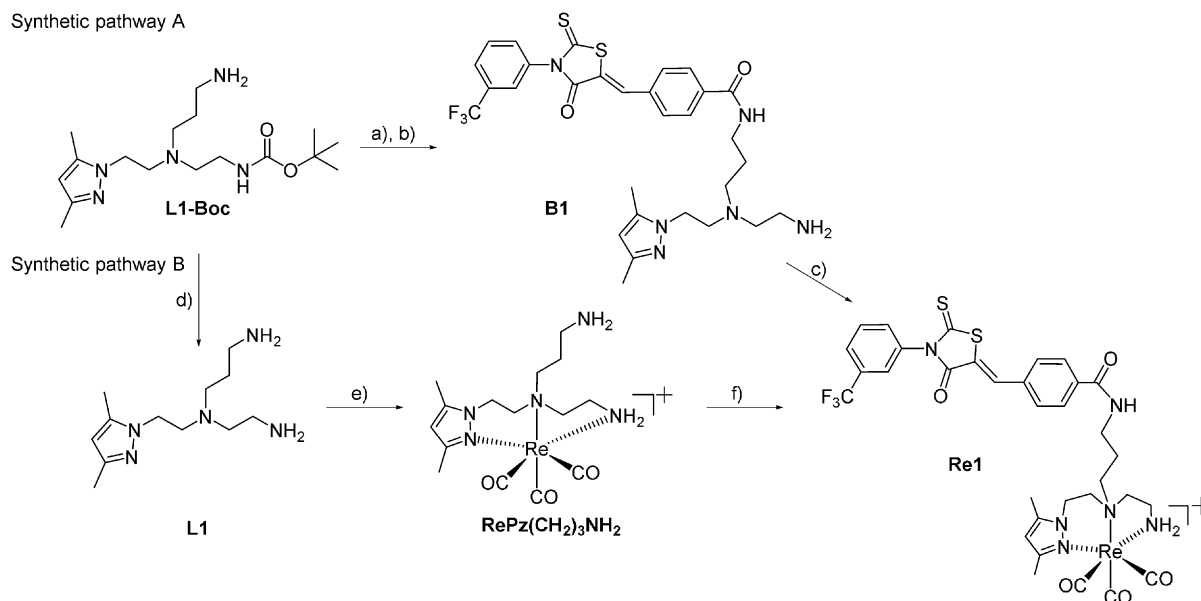
Figure 2. Assessment of **Tc1** stability in fresh human serum. RP-HPLC profile of **Tc1** incubated with fresh human serum for 1 h at 37 °C (γ-detection).

plex proved to be stable in those solutions up to 3 h of incubation.

Functional characterization of the new CFTR-targeting biomolecule

To assess if the structural modifications introduced in CFTR_{inh}-172a upon conjugation to the BFC impaired its ability to recognize CFTR and therefore its ability to inhibit CFTR, we assessed CFTR function in the presence of **Re1** through the iodide efflux technique (Figure 3). This technique is widely used to assay the function of CFTR Cl⁻ channels in intact cells based on the fact that CFTR is also able to permeate other halides.^[29] Briefly, iodide efflux assays start with cell loading with iodide, then activation of CFTR Cl⁻ channels (with forskolin

Synthetic pathway A



Scheme 1. Synthesis of **B1** and Re^I-tricarbonyl complex. Pathway A: a) CFTR_{inh}-172a, HBTU, DIPEA, DMF, room temperature, 4 d, $\eta = 77\%$; b) TFA/CH₂Cl₂ (1:2), room temperature, 2 h, $\eta = 68\%$; c) *fac*-[Re(CO)₃(H₂O)₃]Br, H₂O, reflux, 18 h, $\eta = 55\%$. Pathway B: d) TFA/CH₂Cl₂ (1:2), room temperature, 3 h, $\eta = 54\%$; e) *fac*-[Re(CO)₃(H₂O)₃]Br, H₂O, reflux, 16 h, $\eta = 34\%$; f) CFTR_{inh}-172a, HBTU, DIPEA, DMF, room temperature, 4 d, $\eta = 10\%$.

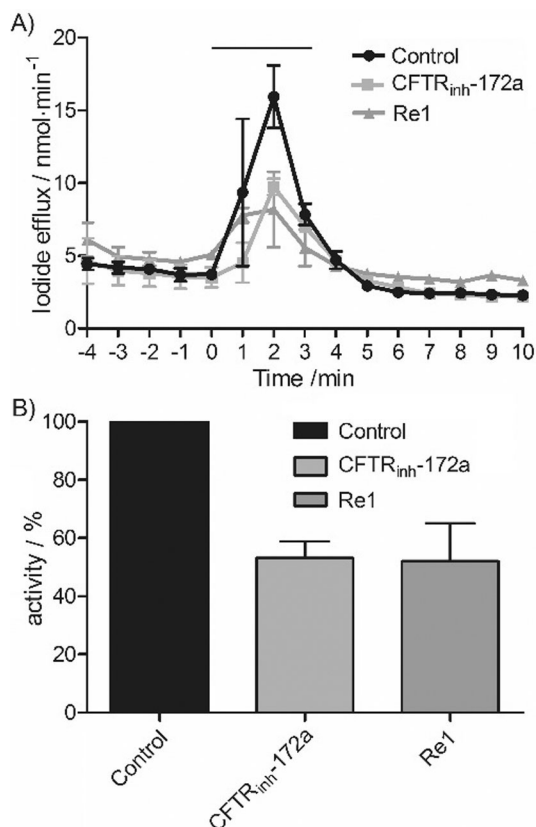


Figure 3. Assessment of CFTR function inhibition by **Re1**. Iodide efflux from BHK cells stably expressing wt CFTR was measured after cell incubation with 25 μM **Re1** or CFTR_{inh}-172a for 15 min. As a control, cells were incubated with 0.25% DMSO. During the period indicated by the solid bar, cells were stimulated with forskolin (10 μM) and genistein (50 μM). A) Time-course of iodide efflux. B) Percentage of CFTR activity at time point 2—maximum iodide efflux—for each assay condition (mean \pm SEM, $n=2-3$).

and genistein, leading to iodide exit from the cell), and assessment of the appearance of iodide in the cell-bathing solutions. For these experiments, we used baby hamster kidney (BHK) cells engineered to stably express high levels of human wild-type (wt) CFTR protein, a well-characterized model system to perform simple functional studies as the one described.

As observed in Figure 3, CFTR activity decreased to approximately half in the presence of CFTR_{inh}-172a (53.1% \pm 5.8). Incubation of wt CFTR cells with **Re1** resulted in 52% of CFTR activity (\pm 13.1), a similar value to the one obtained for the unaltered CFTR_{inh}-172a. These results suggest that the structural modifications introduced in CFTR_{inh}-172a to form an organometallic complex did not affect its inhibitory activity and implicitly its ability to recognize and bind CFTR. This promising result prompted us to explore the potential usefulness of ^{99m}Tc-labeled CFTR_{inh}-172a as an innovative CFTR imaging probe.

Assessment of the ability of Tc1 to detect CFTR at the plasma membrane

With the aim of assessing the ability of **Tc1** to recognize CFTR at the PM of mammalian cells, we first used BHK cells express-

ing both human wt and mutated F508del CFTR protein, which are heterologous cellular models with high levels of CFTR expression. Cells that were not transformed to express CFTR (BHK L) were used as a negative control for CFTR expression. CFTR protein expression in the three mentioned cell lines is shown in Figure 4A. Under normal circumstances, immature CFTR undergoes processing to produce mature CFTR that travels directly to the apical PM. Immature and mature CFTR are clearly distinguishable by their different molecular weight (bands B and C, respectively). In the case of the F508del mutation, CFTR folding is more complex because the phenylalanine residue at position 508 is not present, compromising the overall assembly of the domain in which the residue is inserted. The mutant protein is recognized as misfolded and prematurely degraded and is therefore unable to develop to the mature form.^[30] As observed, mature and immature CFTR protein was detected in wt cells, and only the immature form was detected in F508del CFTR cells. As expected, non-transformed cells did not present CFTR expression.

The ability of **Tc1** to recognize CFTR in BHK cells was tested by uptake assays and the results are shown in Figure 4B. Wild-type CFTR cells presented significantly higher uptake values at

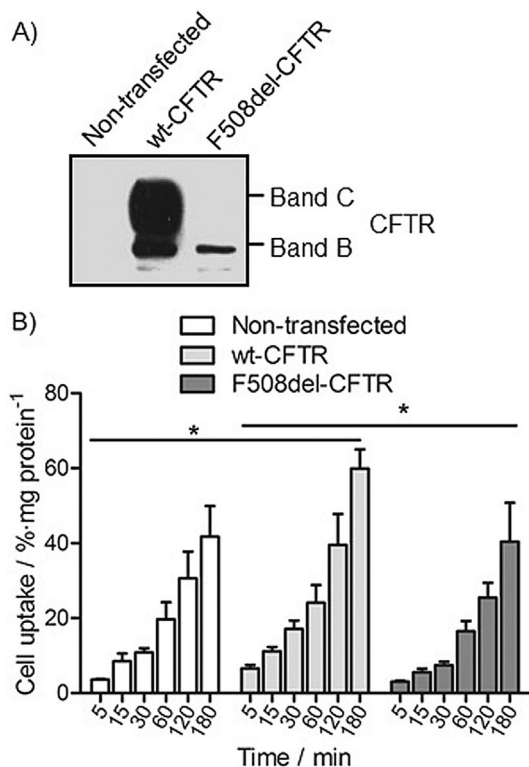


Figure 4. Assessment of **Tc1** uptake in CFTR-expressing and non-expressing BHK cells. A) CFTR expression in BHK cells by western blot. BHK cells stably expressing wt CFTR and F508del CFTR were tested for CFTR expression. Protein extracts samples were loaded at 30 μg of protein per lane. Blots were probed with an antibody specific for CFTR (Ab M3A7). Non-transformed cells (BHK L) were used as a negative control for CFTR expression. B) Cellular uptake of the radioactive complex **Tc1** in BHK cells. Cells were incubated with **Tc1** at 37 $^{\circ}\text{C}$ for up to 180 min. Cellular uptake is expressed as a percentage of radioactivity per milligram of total protein (mean \pm SEM, $n=3$); * $p < 0.05$ considered statistically significant.

all time points compared with mutated F508del CFTR cells (e.g., 6.6 ± 0.9 and 39.6 ± 8.2 versus 3.0 ± 0.3 and 25.5 ± 3.9 for 5 and 120 min, respectively). This can be explained by the fact that wt CFTR is fully processed and able to reach the cell surface, as opposed to F508del CFTR. Nevertheless, the uptake values in F508del CFTR and non-transfected cells were higher than expected, and in fact, not statistically different. This might be due to the lipophilicity of **Tc1** ($\log P = 1.42$) that might bind non-specifically to the PM and diffuse to the intracellular compartment, as observed for other lipophilic cationic ^{99m}Tc complexes,^[31] as well as for CFTR_{inh-172a} itself, which is partially cell permeable.^[32]

Following this first assay in a heterologous model, we then used polarized human CF bronchial epithelial (CFBE) cells, a cellular model that mimics the differentiated state of epithelia. These are immortalized cell lines derived from a CF patient with the F508del mutation but without detectable expression of CFTR, that were subsequently engineered to express either wt or F508del CFTR.

CFBE cells were grown in permeable supports and allowed to polarize, and CFTR expression in wt and F508del CFTR cells was evaluated by western blot (Figure 5A). Again, the presence of mature protein was confirmed for the wt line and only immature protein was observed in the mutant line.

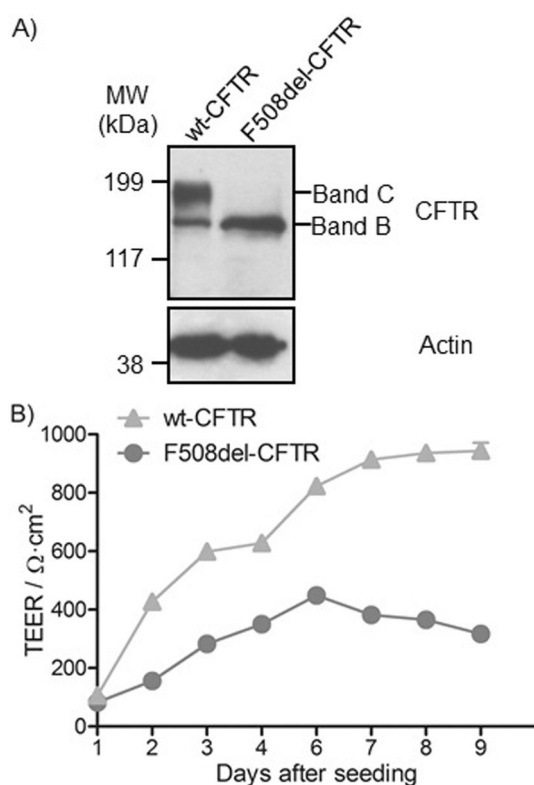


Figure 5. Polarization of CFBE cells. A) CFTR expression in CFBE cells evaluated by western blot. Protein extracts samples were loaded at 30 μg of protein per lane. Blots were probed with an anti-CFTR (Ab 596) and anti-actin antibodies. Molecular weight standards are indicated. B) TEER of polarized CFBE cells. CFBE cells stably expressing wt and F508del CFTR were seeded on filters and allowed to polarize for up to nine days. Polarization was assessed by the measurement of the TEER values (mean \pm SEM, $n = 3-5$).

For assessment of the polarization status of the cultures, we followed the standard methodology of measuring their transepithelial electrical resistance (TEER; Figure 5B). The wt CFTR-expressing cells reached values of TEER close to $1000 \Omega \text{ cm}^2$ after 8–9 days of culture in permeable supports, indicating a fully polarized epithelial cell layer. The lower resistance observed for the monolayer expressing the mutant protein ($\approx 350-400 \Omega \text{ cm}^2$) was expected, and is most likely due to the previously reported delay in differentiation characteristic of the CF epithelium.^[33] In fact, mucus plugging, chronic inflammation, infection, epithelial injury, tissue remodeling, and eventually fibrosis are all hallmarks of CF lung disease.^[34] Similar differences in TEER values have been reported for different airway epithelial cells, such as mutant CFBE41⁰⁻ and normal human bronchial cells (respective values of 250 and $766 \pm 154 \Omega \text{ cm}^2$).^[35]

After polarization, we assessed the ability of **Tc1** to detect CFTR in polarized CFBE cells (Figure 6). In general, the uptake results were in accordance with the obtained for BHK cells. **Tc1** uptake was significantly higher for CFBE cells expressing wt CFTR compared with the mutant F508del CFTR cells, showing that the complex is able to target CFTR at the PM of human polarized epithelia (e.g., 33.3 ± 19.9 and 46.2 ± 14.7 versus 13.7 ± 0.2 and 29.7 ± 3.4 for 60 and 180 min, respectively).

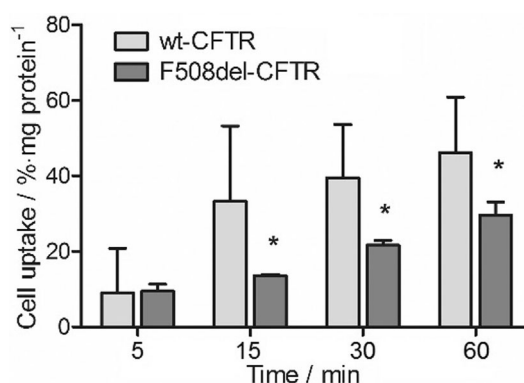


Figure 6. Cellular uptake of the radioactive complex **Tc1** in polarized CFBE cells. Cells were incubated with **Tc1** at 37°C for up to 180 min. Cellular uptake is expressed as a percentage of radioactivity per milligram of total protein (mean \pm SEM, $n = 2-3$); * $p < 0.05$ considered statistically significant.

Assessment of the ability of **Tc1** to detect rescued CFTR at the plasma membrane

Pharmacological correction of mutant CFTR protein can potentially promote protein folding, allowing CFTR to escape premature degradation and reach the PM. One corrector, VX-809, showed great success in vitro^[6] and is currently approved for CF patients with two copies of the F508del mutation in combination with another drug. We performed a western blot analysis of protein extracts of polarized F508del CFTR CFBE cells previously incubated with VX-809 (Figure 7A).

Rescue of F508del CFTR to the PM was observed after treatment with VX-809 (see band C in Figure 7A). Notably, some residual mature form of CFTR was also detected in DMSO-treated

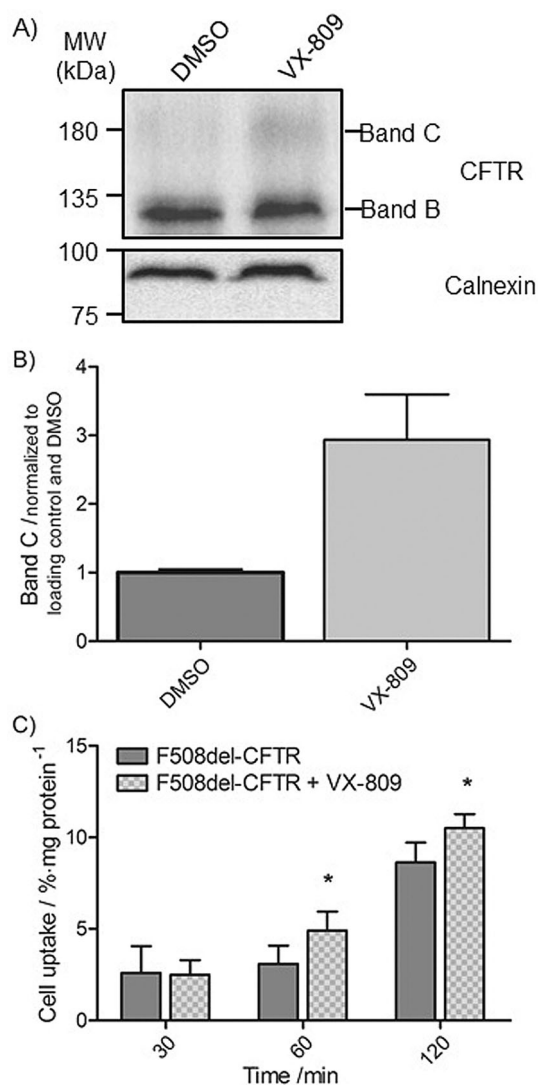


Figure 7. Rescue of F508del CFTR in polarized CFBE cells after treatment with VX-809. CFBE cells stably expressing F508del CFTR were seeded and allowed to polarize. After polarization, cells were incubated with 3 μM VX-809 (and DMSO as negative control) for 48 h at 37 $^{\circ}\text{C}$. A) CFTR expression analysis by western blot. Blots were probed separately with antibodies against CFTR (Ab 596) and calnexin (used as an internal loading control). Molecular weight standards are indicated. B) Band C protein quantification, normalized to loading control and DMSO. C) Cellular uptake of the radioactive complex Tc1. After treatment with VX-809, cells were incubated with Tc1 at 37 $^{\circ}\text{C}$ for up to 120 min. Cellular uptake is expressed as a percentage of radioactivity per milligram of total protein (mean \pm SEM, $n = 2$); * $p < 0.05$ considered statistically significant.

cells (control). DMSO is a chemical chaperone and thus some minor rescuing effect upon F508del CFTR was expected and has been reported previously.^[36] Quantification of the amount of band C revealed approximately three times more fully processed CFTR in VX-809-treated cells comparing with control cells (Figure 7B). Nevertheless, the percentage of mature protein (illustrated by band C) in F508del CFTR corrected cells is only $\approx 15\text{--}20\%$ of wt CFTR band C, as described previously.^[6, 36c]

To fulfil the purpose to which it was envisaged, Tc1 was then used as a probe in the assessment of the pharmacologi-

cal correction of F508del CFTR protein by VX-809 (Figure 7C). At 60 and 120 min, VX-809 led to a significant increase in Tc1 uptake by corrected F508del CFTR cells versus the non-corrected F508del CFTR counterparts (at 120 min, 8.63 ± 0.1 versus 10.5 ± 0.7), in agreement with the trend observed in the western blot analysis, particularly the presence of mature CFTR levels of VX-809-treated cells (Figure 7B). Comparing the two types of experiments, the biochemical assay and the radioactive uptake, we observe that although the amount of fully processed F508del CFTR was threefold higher in the corrected cells, we did not register the same increase in the uptake of Tc1. This can be explained by the fact that fully processed CFTR has to traffic from the Golgi complex via vesicles until the PM, and once there, suffers endocytosis and recycling, and that due to this complex trafficking pathway, not all the fully processed CFTR protein resides at the PM.^[37] Additionally, and as exhibited in the BHK cells, there is possibly some unspecific uptake. In this event, this contribution to the total uptake is not expected to change with the VX-809 treatment and only the specific uptake should correlate to the amount of mature protein.

Preliminary studies of F508del CFTR correction using another chemical corrector—corr-4a—also suggested that the relocation of the mutant protein to the PM can be detected by an increase in Tc1 uptake in corrector-treated F508del CFTR cells (data not shown).

Conclusions

Several image-based assays for the surface expression quantification of F508del CFTR were developed with the potential to be used in the screening for new small molecule F508del CFTR correctors.^[11] However, these assays involve genetically engineering F508del CFTR by fusing it to a fluorophore or a fluorogen-activating protein. Another weakness of these assays is that the fusion proteins are expressed in human embryonic kidney 293 cells, which do not polarize, as opposed to the polarized epithelial cells in which CFTR is mainly expressed.

Herein, we report on the design of a novel probe and the assessment of its targeting ability to detect CFTR at the cell surface in human cells. The probe was based on the CFTR inhibitor CFTR_{inh}-172a, known to interact specifically with CFTR at the region of the channel pore. The radiolabeling strategy involved a three-component system constituted by the biomolecule, a radiometal (^{99m}Tc), and a BFC designed to connect the radiometal to the biomolecule.

The results presented showed that the method described here is sensitive to detect: a) the presence of mature CFTR at the membrane of wt CFTR-expressing bronchial epithelial cells; and, b) the increase in the membrane expression of the protein, as observed for the corrector-treated cells expressing the mutant protein. We cannot exclude that this last observation might be due to the detection of an increase in the total amount of fully glycosylated CFTR, which is then reflected by the presence at the plasma membrane for corrector-rescued F508del CFTR. Notwithstanding, the method is able to discriminate between control and corrector-treated F508del CFTR-ex-

pressing cells thus providing a proof-of-principle validation of our strategy in terms of using a molecular imaging probe.

In the future, we plan to optimize this concept by using a more specific plasma membrane CFTR targeting probe, such as an antibody or antibody fragment, which have been successfully tested for the imaging and therapeutic applications for a variety of targets/diseases.^[38]

Experimental Section

Materials

All chemicals and solvents were of reagent grade and used without purification. Dry *N,N*-dimethylformamide (DMF) was used for reactions in inert atmosphere and dried according to published procedures.^[39] Ligands **L1-Boc** (*tert*-butyl 2-((3-aminopropyl)(2-(3,5-dimethyl-1*H*-pyrazol-1-yl)ethyl)amino)ethylcarbamate) and **L1** (*N*-(2-aminoethyl)-*N*1-(2-(3,5-dimethyl-1*H*-pyrazol-1-yl)ethyl)propane-1,3-diamine), and the organometallic precursor *fac*-[Re(CO)₃(H₂O)₃]Br were prepared according to published methods.^[27b,40] The anti-CFTR antibody 596 was obtained via the CFTR Antibody Distribution Program of the Cystic Fibrosis Foundation Therapeutics (CFFT). The CFTR inhibitor CFTR_{inh}-172a (4-[4-oxo-2-thioxo-3-(3-trifluoromethylphenyl)thiazolidin-5-ylidenemethyl]benzoic acid) was obtained via the Chemical Compound Distribution Program of CFFT. Corrector VX-809 (3-[6-[[1-(2,2-difluoro-1,3-benzodioxol-5-yl)-cyclopropanecarbonyl]amino]-3-methylpyridin-2-yl]benzoic acid) was purchased to Selleck Chemicals (Houston, TX, USA).

General procedures

¹H and ¹³C NMR spectra were recorded at room temperature on a Varian Unity Inova-300 spectrometer (Varian, Agilent Technologies, Santa Clara, CA, USA), with a radiofrequency of 300 and 75.5 MHz, respectively. ¹H and ¹³C chemical shifts (δ) were referenced with the residual solvent resonances relative to tetramethylsilane. The use of 2D NMR experiments (¹H-¹H gCOSY and ¹H-¹³C gHSQC) was essential for peak assignment. All compounds were characterized by MS. Mass spectra were obtained using an EI/quadrupole ion trap mass spectrometer (Bruker HCT, Bruker, Billerica, MA, USA). Mass spectrum of **Re1** was obtained using a MALDI-TOF mass spectrometer (Voyager-DE™ PRO Biospectrometry Workstation, Applied Biosystems, Life Technologies, Foster City, CA, USA) and 2,5-dihydroxybenzoic acid (DHB) as matrix. RP-HPLC analyses were performed on a PerkinElmer Series 200 LC pump (PerkinElmer, Waltham, MA, USA) coupled to an UV/Vis detector (PerkinElmer LC 290 or Shimadzu SPD-10AV, Shimadzu, Kyoto, Japan) and to a γ detector (Berthold-LB 509, Berthold Technologies, Bad Wildbad, BW, Germany). An EC 250/4 Nucleosil 100-10 C₁₈ column (250 × 4 mm, 100 Å pore size, 10 μ m particle size, Macherey-Nagel, Düren, Germany) was used with a flow rate of 1.0 mL min⁻¹. Eluents: A: 0.1% (v/v) trifluoroacetic acid (TFA) in H₂O, B: 0.1% (v/v) TFA in acetonitrile (ACN). Elution method A: *t* = 0–5 min: 20% B; 5–20 min: 20 → 100% B; 20–28 min: 100% B; 28–29 min: 100 → 20% B; 29–30 min: 20% B. For the purification of intermediate **RePz(CH₂)₃NH₂**, a Supelco Discovery BIO Wide Pore C₁₈ column (150 × 10 mm, 300 Å pore size, 10 μ m particle size, Sigma-Aldrich, St. Louis, MO, USA) was used with a flow rate of 3.0 mL min⁻¹. Eluents: A: 0.1% (v/v) TFA in H₂O, B: MeOH. Elution method B: *t* = 0–5 min: 10% B; 5–30 min: 10 → 100% B; 30–34 min: 100% B; 34–35 min: 100 → 10% B; 35–40 min: 10% B.

Purification of compounds by column chromatography was performed using silica-gel 60 with 70–230 mesh granulometry (Merck, Darmstadt, Germany). Sep-Pak C₁₈ chromatography was performed using a Sep-Pak C₁₈® cartridge (360 mg sorbent/cartridge, 125 Å pore size, 55–105 μ m particle size, Waters Co., Milford, MA, USA), preconditioned with MeOH (5.0 mL) and 1 mM HCl (5.0 mL). Elution started with 1 mM HCl (5.0 mL) followed by MeOH (5.0 mL). The presence of the desired compound in the collected fractions was monitored by ¹H NMR spectroscopy. Thin-layer chromatography (TLC) was performed on ALUGRAM® Xtra silica-gel aluminum sheets (Macherey-Nagel) with 0.20 mm of thickness. Compounds were detected with UV light (λ = 254 nm) or revealed with iodine vapor.

Synthesis of (Z)-N-(3-((2-aminoethyl)(2-(3,5-dimethyl-1H-pyrazol-1-yl)ethyl)amino)propyl)-4-((4-oxo-2-thioxo-3-(3-(trifluoromethyl)phenyl)thiazolidin-5-ylidene)methyl)benzamide (B1)

The inhibitor CFTR_{inh}-172a (19.0 mg, 46.4 μ mol), O-(benzotriazol-1-yl)-*N,N,N',N'*-tetramethyluronium hexafluorophosphate (HBTU; 22.0 mg, 58.0 μ mol), and *N,N*-diisopropylethylamine (DIPEA; 43.4 μ L, 249.0 μ mol) were added to a solution of **L1-Boc** (28.0 mg, 82.5 μ mol) in dry DMF (2.0 mL). This reaction mixture was stirred at room temperature for 4 d under N₂. The solvent was removed under vacuum and the resulting product purified by silica gel column chromatography using a gradient of MeOH (4 → 20%) in CHCl₃. The intermediate **B1-Boc** was obtained as a yellow solid (26.0 mg, 77%). ¹H NMR (300 MHz, CDCl₃): δ = 1.41 (9H, s), 1.89 (2H, bs), 2.19 (3H, s), 2.27 (3H, s), 2.64 (2H, bs), 2.75 (2H, bs), 2.92 (2H, bs), 3.12 (2H, bs), 3.48 (2H, bs), 4.16 (2H, bs), 4.96 (1H, bs), 5.87 (1H, s), 7.49–7.59 (4H, m), 7.70 (1H, m), 7.77 (2H, m), 8.15 ppm (2H, d); ¹³C NMR (75.5 MHz, CDCl₃): δ = 11.1, 13.1, 25.1, 28.4, 29.7, 31.2, 36.2, 37.8, 52.1, 53.3, 79.3, 105.6, 124.2, 125.7, 126.6, 126.9, 128.3, 130.1, 130.6, 131.9, 132.8, 135.1, 135.3, 136.3, 138.6, 147.1, 156.0, 166.0, 167.1, 192.5 ppm; MS (EI) (*m/z*) [*M* + H]⁺ calcd for C₃₅H₄₁F₃N₆O₄S₂: 730.9, found: 731.4.

To a solution of the intermediate **B1-Boc** (26.0 mg, 35.6 μ mol) in dichloromethane (2.0 mL) was added TFA (1.0 mL, 13.1 mmol), and this mixture was stirred for 2 h at room temperature. The solvent was removed under vacuum and the resulting product purified by silica gel column chromatography using a gradient of MeOH (10 → 20%) in CHCl₃. **B1** was obtained as a yellow solid (18.0 mg, 68%). ¹H NMR (300 MHz, CD₃OD): δ = 1.62 (2H, quint), 2.18 (3H, s), 2.27 (3H, s), 2.54 (2H, t), 2.75–2.86 (4H, m), 3.01 (2H, t), 3.25 (2H, t), 4.09 (2H, t), 5.85 (1H, s), 7.64–7.86 (7H, m), 7.98 ppm (2H, d); ¹³C NMR (75.5 MHz, CD₃OD): δ = 11.0, 13.3, 28.3, 38.5, 39.0, 47.5, 52.4, 52.6, 54.4, 106.4, 126.7, 125.1, 127.2, 127.5, 129.3, 131.5, 131.7, 132.7, 132.9, 133.9, 137.2, 137.3, 137.6, 141.1, 148.5, 168.6, 169.0, 194.9 ppm; MS (EI) (*m/z*) [*M* + H]⁺ calcd for C₃₀H₃₃F₃N₆O₂S₂: 630.2, found: 631.4; *t*_R = 17.6 min (λ = 220 nm).

Synthesis of Re complex *fac*-[Re(CO)₃(κ^3 -B1)]⁺ (Re1)

Synthetic pathway A: The precursor *fac*-[Re(CO)₃(H₂O)₃]Br (12.5 mg, 30.9 μ mol) was added to a solution of **B1** (20.0 mg, 26.8 μ mol) in water (5.0 mL). Following neutralization with 2.5 M NaOH, the solution was held at reflux for 18 h. **Re1** was obtained as a yellow precipitate, isolated by decantation, and washed several times with water, hexane, and dichloromethane (13.3 mg, 55%). ¹H NMR (300 MHz, CD₃OD): δ = 2.16–2.29 (2H, m), 2.35 (3H, s), 2.44 (3H, s), 2.55 (1H, m), 2.72 (2H, m), 2.85 (2H, m), 3.17 (2H, m), 3.54 (2H, t), 3.78 (1H, m), 4.09 (1H, bs), 4.24 (1H, m), 4.51 (1H, dd), 5.54

(1H, bs), 6.20 (1H, s), 7.65–7.86 (7H, m), 8.00 ppm (2H, d); ^{13}C NMR (75.5 MHz, CD_3OD): $\delta = 11.6, 16.1, 25.9, 30.8, 38.7, 43.8, 54.3, 63.0, 66.3, 109.3, 126.8, 127.2, 127.5, 129.3, 129.7, 131.7, 132.6, 134.0, 137.0, 137.4, 137.7, 145.4, 155.2, 168.6, 169.4, 193.8, 194.9, 195.3, 198.2$ ppm; MALDI/TOF-MS m/z [M] $^+$ calcd for $\text{C}_{33}\text{H}_{33}\text{F}_3\text{N}_6\text{O}_5\text{ReS}_2$: 901.2, found: 901.1.

Synthetic pathway B: To a solution of **L1** (42.5 mg, 90.5 μmol) in water (10 mL) was added the *fac*- $[\text{Re}(\text{CO})_3(\text{H}_2\text{O})_3]\text{Br}$ precursor (42.1 mg, 104.1 μmol). The solution was neutralized with 2.5 M NaOH and held at reflux for 16 h. After purification by RP-HPLC (elution method B), **RePz**(CH_2) $_3\text{NH}_2$ was obtained as a colorless oil (15.7 mg, 34%). ^1H NMR (300 MHz, D_2O): $\delta = 2.14$ (2H, m), 2.30 (3H, s), 2.41 (3H, s), 2.57 (1H, m), 2.72 (1H, m), 2.88 (2H, m), 3.08 (2H, t), 3.21 (1H, m), 3.42 (1H, dd), 3.52 (1H, td), 3.76 (2H, m), 4.24 (1H, m), 4.46 (1H, dd), 5.24 (1H, bs), 6.18 ppm (1H, s); ^{13}C NMR (75.5 MHz, D_2O): $\delta = 10.7, 15.2, 22.3, 37.0, 42.1, 46.8, 52.5, 61.0, 62.9, 107.7, 144.2, 153.7, 192.7, 193.8, 194.4$ ppm; MS (EI) m/z [$M + \text{H}$] $^+$ calcd for $\text{C}_{15}\text{H}_{25}\text{N}_5\text{O}_3\text{Re}$: 509.6, found: 510.3.

To a solution of **RePz**(CH_2) $_3\text{NH}_2$ (15.7 mg, 30.8 μmol) in dry DMF (2.0 mL) were added the inhibitor CFTR $_{\text{inh}}$ -172a (7.0 mg, 17.1 μmol), HBTU (8.1 mg, 21.4 μmol), and DIPEA (15.1 μL , 92.4 μmol). The reaction mixture was stirred at room temperature for 4 d under N_2 . The solvent was removed under vacuum and the resulting product purified by Sep-Pak C_{18} chromatography using 1.0 mm HCl and MeOH. After evaporation of the solvents from the collected fractions, **Re1** was obtained as a yellow solid (1.5 mg, 10%). ^1H NMR (300 MHz, CD_3OD): $\delta = 2.21$ –2.32 (2H, m), 2.37 (3H, s), 2.45 (3H, s), 2.54 (1H, m), 2.72 (2H, m), 2.82 (2H, m), 3.17 (2H, m), 3.54 (2H, t), 3.79 (1H, m), 4.09 (1H, bs), 4.24 (1H, m), 4.52 (1H, dd), 5.53 (1H, bs), 6.22 (1H, s), 7.64–7.87 (7H, m), 8.01 ppm (2H, d); MS (EI) m/z [$M + \text{H}$] $^+$ calcd for $\text{C}_{33}\text{H}_{33}\text{F}_3\text{N}_6\text{O}_5\text{ReS}_2$: 901.2, found: 901.5; $t_{\text{R}} = 24.5$ min ($\lambda = 254$ nm); purity determined by RP-HPLC $\geq 95\%$.

Synthesis and characterization of the $^{99\text{m}}\text{Tc}$ complex **Tc1**

Preparation of the *fac*- $[\text{fac-}^{99\text{m}}\text{Tc}(\text{H}_2\text{O})_3(\text{CO})_3]^+$ precursor: Saline solution was used to elute pertechnetate ($[\text{fac-}^{99\text{m}}\text{TcO}_4]^-$) from a $^{99}\text{Mo}/^{99\text{m}}\text{Tc}$ generator. Approximately 2.0 mL of the eluate were added to an IsoLink $^{\text{®}}$ kit (Mallinckrodt-Covidien, Petten, The Netherlands) containing the following lyophilized formulation: sodium tetraborate decahydrate (2.85 mg), sodium boranocarbonate (4.50 mg), sodium carbonate (7.15 mg) and sodium tartrate dihydrate (8.50 mg). The reaction vial was incubated at 100 $^{\circ}\text{C}$ for 30 min and the solution neutralized with 1 M HCl (≈ 140.0 μL) to decompose any residual boranocarbonate. The precursor formation was followed by RP-HPLC (γ -detection).

Radiolabeling of B1 with the *fac*- $[\text{fac-}^{99\text{m}}\text{Tc}(\text{CO})_3]^+$ core: The precursor *fac*- $[\text{fac-}^{99\text{m}}\text{Tc}(\text{H}_2\text{O})_3(\text{CO})_3]^+$ in 0.9% (w/v) NaCl (≈ 1 mCi) was added to a capped nitrogen-purged glass vial containing a 10^{-3} M aqueous solution of **B1** (final concentration = 10^{-4} M). The reaction vial was incubated at 50 $^{\circ}\text{C}$ for 30 min, cooled, and the solution analyzed and purified by RP-HPLC (γ -detection); $t_{\text{R}} = 25.1$ min; purity determined by RP-HPLC $\geq 95\%$.

In vitro stability: 100 μL of **Tc1** were incubated with 500 μL of fresh human serum and cell medium (used in the biological assays) at 37 $^{\circ}\text{C}$ for up to 3 h. The stability of the $^{99\text{m}}\text{Tc}$ complex was analyzed by RP-HPLC (γ -detection).

Partition coefficient: The lipophilicity of **Tc1** was evaluated by determining the partition coefficient in the biphasic system *n*-octanol/0.1 M PBS pH 7.4 ($P_{\text{o/w}}$). A mixture of octanol and 0.1 M PBS pH 7.4 (1:1, v/v) was prepared and stirred for 1 min. **Tc1** (25 μL)

was added and the mixture vortexed for 1 min and centrifuged (1700 g , 10 min, room temperature) to allow phase separation. After centrifugation, both phases were separated and aliquots of each collected and counted in a γ -counter; 500 μL of the organic phase were collected and further extracted with 500 μL of 0.1 M PBS pH 7.4. Four replicates were used in the experiment. $P_{\text{o/w}}$ is determined as the ratio between the organic and the aqueous phases. The results were expressed as $\log P$; $\log P$ **Tc1** = 1.42.

Cell lines and cell culture conditions: BHK cells (kindly provided by Prof G. Lukacs, McGill University, Montr al, QC, Canada) and CFBE cells stably expressing either wt or F508del CFTR (kindly provided by the Gregory Fleming James Cystic Fibrosis Research Center at the University of Alabama at Birmingham, AL, and Prof D. Gruenert, University of California at San Francisco, CA, USA) were used in the experiments. Cells were grown in plastic culture flasks at 37 $^{\circ}\text{C}$ in a humidified atmosphere of 5% CO_2 . Transfected BHK cells were cultured in a 1:1 mixture of Dulbecco's modified Eagle's medium and Ham's F-12 nutrient medium (DMEM/F-12) supplemented with 5% heat-inactivated fetal bovine serum (FBS), 1% penicillin/streptomycin (all from Gibco, Thermo Fisher Scientific, Waltham, MA USA), and 0.2% methotrexate (Sigma–Aldrich, omitted from the media used to grow non-transfected BHK cells). CFBE cells were cultured in minimal essential medium (MEM, Gibco, Thermo Fisher Scientific) supplemented with 10% FBS, 1% penicillin/streptomycin, and 2.5 $\mu\text{g mL}^{-1}$ puromycin (Sigma–Aldrich). Two to three days before the assays, the selection agent was removed from the media. For experiments requiring polarization conditions to mimic the differentiated state of epithelia, CFBE cells were seeded onto 12- and 24-well Corning Transwell $^{\text{®}}$ Permeable Supports (Corning, NY, USA) at a density of 2.5×10^5 and 8.8×10^4 cells per well, respectively. Prior to seeding, the supports were coated with collagen IV (Sigma–Aldrich). For the initial seeding, cells were cultured in MEM supplemented with 10% FBS. On the following day, the percentage of FBS was decreased to 2%. The medium was changed every second day to maintain the cells until the day of the experiment. To follow polarization, TEER values were measured using the STX2 Electrode coupled to the EVOM 2 Epithelial Voltohmmeter (World Precision Instruments, Hitchin, HFD, UK). For the modulation studies, polarized CFBE cells were pre-incubated (48 h) with 3 μM VX-809 (in DMSO) at 37 $^{\circ}\text{C}$. As a negative control, cells were pre-incubated with the same percentage of DMSO.

Iodide efflux: Iodide efflux experiments were performed as previously described. $^{[29a]}$ BHK stably expressing human wt CFTR cells were seeded in 60 mm plastic culture dishes and media changed every second day. The experiments were performed when culture dishes were 80–90% confluent (approximately after four days). Cells were incubated with iodide-loading buffer (containing in mM: 136 NaI, 3 KNO_3 , 2 $\text{Ca}(\text{NO}_3)_2$, 20 HEPES, and 11 glucose, pH 7.4) at room temperature in the dark for 1 h. Cells were then washed ten times with efflux buffer (equal to loading buffer but with NaNO_3 replacing NaI) to remove iodide from the cell-bathing solution. From this point, CFTR $_{\text{inh}}$ -172a and **Re1** were present in the efflux buffer until the end of the experiment (time point –4 to 10). Stock solutions of 10 mM CFTR $_{\text{inh}}$ -172a and **Re1** in DMSO were prepared and the compounds used at a final concentration of 25 μM (0.25% DMSO). As a control, cells were incubated with efflux buffer containing 0.25% DMSO. To start the assay, fresh efflux buffer was added to each culture dish and cells were allowed to equilibrate. After 1 min, the efflux buffer was collected and fresh efflux buffer was added. These steps were repeated at 1-min intervals (time point –4 to –1). Efflux buffer containing 10 μM forskolin and 50 μM genistein (Sigma–Aldrich) was added for 4 min to stimulate

CFTR Cl⁻ channels (time point 0 to 3). Finally, fresh efflux buffer was added until the end of the experiment (time point 4 to 10). The amount of iodide in each collected sample of efflux buffer (unexposed to light) was determined using an iodide-sensitive electrode (ThermoElectron Corporation, Thermo Fisher Scientific). The assay was performed using at least two replicates for each condition.

Western blot: BHK or CFBE cells were lysed using the CellLytic M lysis/extraction reagent (Sigma–Aldrich) supplemented with a cOmplete™ Protease Inhibitor Cocktail tablet (Roche Applied Science, Penzberg, Upper Bavaria, Germany).^[41] After 15-min incubation at 4 °C with regular shaking, lysates were centrifuged at 14000 g for 20 min to pellet the cellular debris, and the protein-containing supernatants collected and properly stored. Total protein content from each sample was determined using the DCTM Protein Assay kit (BioRad Laboratories, Hercules, CA, USA). Samples were diluted in sample buffer [31.25 mM Tris (pH 6.8), 1.5% (w/v) sodium dodecyl sulfate (SDS), 10% (v/v) glycerol, 0.001% (w/v) bromophenol blue, 0.5 mM dithiothreitol] and incubated in a water bath at 37 °C for 15 min; 30 µg of total protein were loaded per lane and separated in a 7% (w/v) polyacrylamide gel by SDS-polyacrylamide gel electrophoresis (PAGE) using the MiniProtean® Cell (BioRad). Molecular weight standards were also loaded. Proteins were then transferred onto nitrocellulose membranes (Protan® BA85, GE Healthcare Life Sciences, Chicago, IL, USA) using the Mini Trans-Blot® (BioRad) and the blots blocked with 5% (w/v) nonfat dry milk in 0.1% (v/v) phosphate buffer saline-Tween 20 (PBS-T) for 2 h. Blots were incubated separately with the anti-CFTR antibodies M3A7 (dilution 1:1000, ThermoFisher) or 596 (dilution 1:3000) for 1 h, and when an internal control was needed, with an antibody anti-calnexin (dilution 1:3000, BD Biosciences, San Jose, CA, USA) or anti-actin (dilution 1:15000, Sigma). After three 10-min washes with 0.1% (v/v) PBS-T, blots were incubated for 1 h with a secondary antibody (goat anti-mouse IgG-HRP conjugate, dilution 1:3000, BioRad), washed three times with 0.1% (v/v) PBS-T, and developed using the SuperSignal™ West Pico Substrate kit (Pierce, Thermo Fisher Scientific).

Cellular uptake of ^{99m}Tc complex Tc1: Cellular uptake assays were performed in 24-well tissue culture plates. BHK cells were seeded at a density of 1.5 × 10⁵ cells per well in complete culture medium and allowed to attach overnight. Polarized CFBE cells were seeded as described above. On the day of the assay, the culture medium was removed and cells were incubated with Tc1 (≈ 1 µCi per mL of assay medium) at 37 °C. For polarized CFBE cells, assay medium was added only to the upper compartment, while the lower was loaded with medium without Tc1. Incubation was terminated at different time points by removing the medium containing the radioactive complex and washing cells twice with ice-cold PBS. Subsequently, cells were lysed by incubation with 1 M NaOH at 37 °C for 10 min, and in the case of polarized CFE cells, 0.1 M NaOH. The activity of lysates was measured in a γ-counter (Berthold-LB 211, Berthold Technologies). Uptake studies were performed at least in duplicate assays with two or more replicates for each time point. Final results were normalized for protein content. Total protein was determined using the DCTM Protein Assay kit. When appropriate, Student's *t*-test was performed, with *p* < 0.05 considered as the level of statistical significance.

Acknowledgements

This work was funded by grants EXPL/BIM-MEC/0115/2012 (to F.M.) and UID/Multi/04349/2013 (to C²TN) and PEst-OE/BIA/UI4046/2011 (to BioISI) from Fundação para a Ciência e Tecnologia (FCT), Portugal. FCT is also acknowledged for fellowships SFRH/BD/108623/2015 to V.F.C.F., SFRH/BD/38753/2007 to B.L.O., and PD/BD/106084/2015 to J.D.S., and for the FCT Investigator grant to F.M.. EI-MS analyses were carried out on a QITMS instrument, acquired with the support of Programa Nacional de Reequipamento Científico (Contract REDE/1503/REM/2005-ITN) of FCT, part of RNEM-Rede Nacional de Espectrometria de Massa. MALDI/TOF-MS data were obtained at the Laboratório de Análises/Requimte of the Departamento de Química da Universidade Nova de Lisboa. The authors thank the Cystic Fibrosis Foundation Therapeutics for providing the CFTR inhibitor CFTR_{inh}-172a and antibody 596 through the Chemical Compound Distribution Program and CFTR Antibody Distribution Program, respectively.

Conflict of interest

The authors declare no conflict of interest.

Keywords: CFTR • cystic fibrosis • imaging agents • radiopharmaceuticals • technetium

- [1] J. R. Riordan, J. M. Rommens, B. Kerem, N. Alon, R. Rozmahel, Z. Grzelczak, J. Zielenski, S. Lok, N. Plavsic, J. L. Chou, et al., *Science* **1989**, *245*, 1066–1073.
- [2] a) S. H. Cheng, R. J. Gregory, J. Marshall, S. Paul, D. W. Souza, G. A. White, C. R. O'Riordan, A. E. Smith, *Cell* **1990**, *63*, 827–834; b) D. Penque, F. Mendes, S. Beck, C. Farinha, P. Pacheco, P. Nogueira, J. Lavinha, R. Malho, M. D. Amaral, *Lab Invest.* **2000**, *80*, 857–868.
- [3] a) G. M. Denning, M. P. Anderson, J. F. Amara, J. Marshall, A. E. Smith, M. J. Welsh, *Nature* **1992**, *358*, 761–764; b) S. Sato, C. L. Ward, M. E. Krouse, J. J. Wine, R. R. Kopito, *J. Biol. Chem.* **1996**, *271*, 635–638.
- [4] a) M. Sharma, F. Pampinella, C. Nemes, M. Benharouga, J. So, K. Du, K. G. Bache, B. Papsin, N. Zerangue, H. Stenmark, G. L. Lukacs, *J. Cell Biol.* **2004**, *164*, 923–933; b) A. Swiatecka-Urban, A. Brown, S. Moreau-Marquis, J. Renuka, B. Coutermarsh, R. Barnaby, K. H. Karlson, T. R. Flotte, M. Fukuda, G. M. Langford, B. A. Stanton, *J. Biol. Chem.* **2005**, *280*, 36762–36772.
- [5] W. Dalemans, P. Barbry, G. Champigny, S. Jallat, K. Dott, D. Dreyer, R. G. Crystal, A. Pavirani, J. P. Lecocq, M. Lazdunski, *Nature* **1991**, *354*, 526–528.
- [6] F. Van Goor, S. Hadida, P. D. Grootenhuys, B. Burton, J. H. Stack, K. S. Straley, C. J. Decker, M. Miller, J. McCartney, E. R. Olson, J. J. Wine, R. A. Frizzell, M. Ashlock, P. A. Negulescu, *Proc. Natl. Acad. Sci. USA* **2011**, *108*, 18843–18848.
- [7] J. P. Clancy, S. M. Rowe, F. J. Accurso, M. L. Aitken, R. S. Amin, M. A. Ashlock, M. Ballmann, M. P. Boyle, I. Bronsveld, P. W. Campbell, K. De Boeck, S. H. Donaldson, H. L. Dorkin, J. M. Dunitz, P. R. Durie, M. Jain, A. Leonard, K. S. McCoy, R. B. Moss, J. M. Pilewski, D. B. Rosenbluth, R. C. Rubenstein, M. S. Schechter, M. Botfield, C. L. Ordonez, G. T. Spencer-Green, L. Vernillet, S. Wisseh, K. Yen, M. W. Konstan, *Thorax* **2012**, *67*, 12–18.
- [8] C. E. Wainwright, J. S. Elborn, B. W. Ramsey, G. Marigowda, X. Huang, M. Cipolli, C. Colombo, J. C. Davies, K. De Boeck, P. A. Flume, M. W. Konstan, S. A. McColley, K. McCoy, E. F. McKone, A. Munck, F. Ratjen, S. M. Rowe, D. Waltz, M. P. Boyle, *New Engl. J. Med.* **2015**, *373*, 220–231.
- [9] J. L. Taylor-Cousar, J. Lekstrom-Himes, L. Wang, Y. Lu, S. Elborn, *Pediatric Pulmonology* **2017**, *52*, S307.

- [10] a) K. De Boeck, L. Kent, J. Davies, N. Derichs, M. Amaral, S. M. Rowe, P. Middleton, H. de Jonge, I. Bronsveld, M. Wilschanski, P. Melotti, I. Danner-Boucher, S. Boerner, I. Fajac, K. Southern, R. A. de Nooijer, A. Bot, Y. de Rijke, E. de Wachter, T. Leal, F. Vermeulen, M. J. Hug, G. Rault, T. Nguyen-Khoa, C. Barreto, M. Proesmans, I. Sermet-Gaudelus, *Eur. Respir. J.* **2013**, *41*, 203–216; b) S. C. Bell, K. De Boeck, M. D. Amaral, *Pharmacol. Ther.* **2015**, *145*, 19–34.
- [11] a) J. P. Holleran, M. L. Glover, K. W. Peters, C. A. Bertrand, S. C. Watkins, J. W. Jarvik, R. A. Frizzell, *Mol. Med.* **2012**, *18*, 685–696; b) M. B. Larsen, J. Hu, R. A. Frizzell, S. C. Watkins, *Methods* **2016**, *96*, 40–45; c) E. Langron, M. I. Simone, C. M. Delalande, J. L. Reymond, D. L. Selwood, P. Vergani, *Br. J. Pharmacol.* **2017**, *174*, 525–539.
- [12] a) K. Glunde, A. P. Pathak, Z. M. Bhujwala, *Trends Mol. Med.* **2007**, *13*, 287–297; b) M. L. James, S. S. Gambhir, *Physiol. Rev.* **2012**, *92*, 897–965.
- [13] a) R. Alberto, R. Schibli, A. Egli, A. P. Schubiger, U. Abram, T. A. Kaden, *J. Am. Chem. Soc.* **1998**, *120*, 7987–7988; b) M. Morais, A. Paulo, L. Gano, I. Santos, J. D. G. Correia, *J. Organomet. Chem.* **2013**, *744*, 125–139.
- [14] R. Schibli, R. La Bella, R. Alberto, E. Garcia-Garayoa, K. Ortner, U. Abram, P. A. Schubiger, *Bioconjugate Chem.* **2000**, *11*, 345–351.
- [15] R. Waibel, R. Alberto, J. Willuda, R. Finnern, R. Schibli, A. Stichelberger, A. Egli, U. Abram, J. P. Mach, A. Pluckthun, P. A. Schubiger, *Nat. Biotechnol.* **1999**, *17*, 897–901.
- [16] M. Klein, M. Cohen-Cymbarknoh, S. Armoni, D. Shoseyov, R. Chisin, M. Orevi, N. Freedman, E. Kerem, *Chest* **2009**, *136*, 1220–1228.
- [17] M. Lindstrom, P. Camner, R. Falk, L. Hjelte, K. Philipson, M. Svartengren, *Eur. Respir. J.* **2005**, *25*, 317–323.
- [18] J. A. Kastelik, G. A. Wright, I. Aziz, M. Davies, G. R. Avery, A. J. Paddon, S. Howey, A. H. Morice, *Pulm Pharmacol. Ther.* **2002**, *15*, 513–519.
- [19] T. Ma, J. R. Thiagarajah, H. Yang, N. D. Sonawane, C. Folli, L. J. Galiotta, A. S. Verkman, *J. Clin. Invest.* **2002**, *110*, 1651–1658.
- [20] E. Caci, A. Caputo, A. Hinzpeter, N. Arous, P. Fanen, N. Sonawane, A. S. Verkman, R. Ravazzolo, O. Zegarra-Moran, L. J. Galiotta, *Biochem. J.* **2008**, *413*, 135–142.
- [21] I. Virgolini, C. Decristoforo, A. Haug, S. Fanti, C. Uprimny, *Eur. J. Nucl. Med. Mol. Imaging* **2018**, *45*, 471–495.
- [22] M. Fani, G. P. Nicolas, D. Wild, *J. Nucl. Med.* **2017**, *58*, 615–665.
- [23] A. M. E. Walenkamp, C. Lapa, K. Herrmann, H. J. Wester, *J. Nucl. Med.* **2017**, *58*, 775–825.
- [24] a) M. Ginj, H. Zhang, B. Waser, R. Cescato, D. Wild, X. Wang, J. Erchegyi, J. Rivier, H. R. Macke, J. C. Reubi, *Proc. Natl. Acad. Sci. USA* **2006**, *103*, 16436–16441; b) D. Wild, M. Fani, M. Behe, I. Brink, J. E. Rivier, J. C. Reubi, H. R. Maecke, W. A. Weber, *J. Nucl. Med.* **2011**, *52*, 1412–1417; c) J. C. Reubi, J. Erchegyi, R. Cescato, B. Waser, J. E. Rivier, *Eur. J. Nucl. Med. Mol. Imaging* **2010**, *37*, 1551–1558.
- [25] a) M. D. Bartholomä, A. S. Louie, J. F. Valliant, J. Zubieta, *Chem. Rev.* **2010**, *110*, 2903–2920; b) S. Liu, *Chem. Soc. Rev.* **2004**, *33*, 445–461.
- [26] a) P. Nunes, G. R. Morais, E. Palma, F. Silva, M. C. Oliveira, V. F. C. Ferreira, F. Mendes, L. Gano, H. V. Miranda, T. F. Outeiro, I. Santos, A. Paulo, *Org. Biomol. Chem.* **2015**, *13*, 5182–5194; b) M. Morais, V. F. C. Ferreira, F. Figueira, F. Mendes, P. Raposinho, I. Santos, B. L. Oliveira, J. D. G. Correia, *Dalton Trans.* **2017**, *46*, 14537–14547.
- [27] a) S. Alves, A. Paulo, J. D. G. Correia, L. Gano, C. J. Smith, T. J. Hoffman, I. Santos, *Bioconjugate Chem.* **2005**, *16*, 438–449; b) R. F. Vitor, S. Alves, J. D. G. Correia, A. Paulo, I. Santos, *J. Organomet. Chem.* **2004**, *689*, 4764–4774; c) M. Morais, P. D. Raposinho, M. C. Oliveira, D. Pantoja-Uceda, M. A. Jiménez, I. Santos, J. D. G. Correia, *Organometallics* **2012**, *31*, 5929–5939.
- [28] a) S. Alves, A. Paulo, J. D. G. Correia, A. Domingos, I. Santos, *J. Chem. Soc. Dalton Trans.* **2002**, 4714–4719; b) B. L. Oliveira, P. D. Raposinho, F. Mendes, F. Figueira, I. Santos, A. Ferreira, C. Cordeiro, A. P. Freire, J. D. Correia, *Bioconjugate Chem.* **2010**, *21*, 2168–2172.
- [29] a) A. Schmidt, L. K. Hughes, Z. Cai, F. Mendes, H. Li, D. N. Sheppard, M. D. Amaral, *Br. J. Pharmacol.* **2009**, *153*, 1311–1323; b) M. Roxo-Rosa, Z. Xu, A. Schmidt, M. Neto, Z. Cai, C. M. Soares, D. N. Sheppard, M. D. Amaral, *Proc. Natl. Acad. Sci. USA* **2006**, *103*, 17891–17896.
- [30] C. M. Farinha, M. D. Amaral, *Mol. Cell. Biol.* **2005**, *25*, 5242–5252.
- [31] a) S. Liu, *Dalton Trans.* **2007**, 1183–1193; b) C. Moura, F. Mendes, L. Gano, I. Santos, A. Paulo, *J. Inorg. Biochem.* **2013**, *123*, 34–45.
- [32] A. S. Verkman, D. Synder, L. Tradtrantip, J. R. Thiagarajah, M. O. Anderson, *Curr. Pharm. Des.* **2013**, *19*, 3529–3541.
- [33] J. E. Larson, J. B. Delcarpio, M. M. Farberman, S. L. Morrow, J. C. Cohen, *Am. J. Physiol.* **2000**, *279*, L333–341.
- [34] R. Hajj, P. Lesimple, B. Nawrocki-Raby, P. Birembaut, E. Puchelle, C. Coraux, *J. Pathol.* **2007**, *211*, 340–350.
- [35] B. Srinivasan, A. R. Kolli, M. B. Esch, H. E. Abaci, M. L. Shuler, J. J. Hickman, *J. Lab. Autom.* **2015**, *20*, 107–126.
- [36] a) N. Pedemonte, G. L. Lukacs, K. Du, E. Caci, O. Zegarra-Moran, L. J. Galiotta, A. S. Verkman, *J. Clin. Invest.* **2005**, *115*, 2564–2571; b) K. Varga, R. F. Goldstein, A. Jurkuvenaite, L. Chen, S. Matalon, E. J. Sorscher, Z. Bebok, J. F. Collawn, *Biochem. J.* **2008**, *410*, 555–564; c) C. M. Farinha, J. King-Underwood, M. Sousa, A. R. Correia, B. J. Henriques, M. Roxo-Rosa, A. C. Da Paula, J. Williams, S. Hirst, C. M. Gomes, M. D. Amaral, *Chem. Biol.* **2013**, *20*, 943–955.
- [37] K. Varga, A. Jurkuvenaite, J. Wakefield, J. S. Hong, J. S. Guimbellot, C. J. Venglarik, A. Niraj, M. Mazur, E. J. Sorscher, J. F. Collawn, Z. Bebok, *J. Biol. Chem.* **2004**, *279*, 22578–22584.
- [38] a) R. Chakravarty, S. Goel, H. F. Valdovinos, R. Hernandez, H. Hong, R. J. Nickles, W. Cai, *Bioconjugate Chem.* **2014**, *25*, 2197–2204; b) K. Steinhoff, M. Pierer, J. Siegert, U. Pigla, R. Laub, S. Hesse, W. Seidel, D. Sorger, A. Seese, J. U. Kuenstler, H. J. Pietzsch, T. Lincke, M. Rullmann, F. Emmrich, O. Sabri, *Nucl. Med. Biol.* **2014**, *41*, 350–354; c) S. Lütje, C. M. van Rij, G. M. Franssen, G. Fracasso, W. Helfrich, A. Eek, W. J. Oyen, M. Colombatti, O. C. Boerman, *Contrast Media Mol. Imaging* **2015**, *10*, 28–36.
- [39] W. L. F. Armarego, C. Chai in *Purification of Laboratory Chemicals, 7th ed.*, Butterworth-Heinemann, Boston, **2013**, pp. 103–554.
- [40] N. Lazarova, S. James, J. Babich, J. Zubieta, *Inorg. Chem. Commun.* **2004**, *7*, 1023–1026.
- [41] a) C. M. Farinha, P. Nogueira, F. Mendes, D. Penque, M. D. Amaral, *Biochem. J.* **2002**, *366*, 797–806; b) F. Mendes, J. Wakefield, T. Bachhuber, M. Barroso, Z. Bebok, D. Penque, K. Kunzelmann, M. D. Amaral, *Cell Physiol. Biochem.* **2005**, *16*, 281–290; c) A. S. Ramalho, M. A. Lewandowska, C. M. Farinha, F. Mendes, J. Goncalves, C. Barreto, A. Harris, M. D. Amaral, *Cell. Physiol. Biochem.* **2009**, *24*, 335–346.

Manuscript received: March 21, 2018

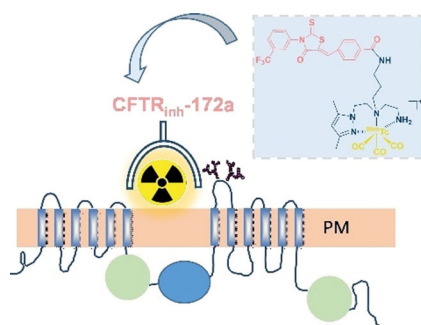
Revised manuscript received: May 18, 2018

Accepted manuscript online: June 4, 2018

Version of record online: ■ ■ ■ ■ ■ 0000

FULL PAPERS

Molecular imaging of CF: Cystic fibrosis, the most common lethal autosomal recessive disorder in Caucasians, is caused by mutations in the CF transmembrane conductance regulator (CFTR) gene, which encodes an epithelial chloride channel. Herein, we describe the development of the first specific imaging probe to allow detection of CFTR in vivo, based on a new technetium complex and a targeting biomolecule.



V. F. C. Ferreira, B. L. Oliveira, J. D. Santos,
J. D. G. Correia, C. M. Farinha, F. Mendes*



**Targeting of the Cystic Fibrosis
Transmembrane Conductance
Regulator (CFTR) Protein with a
Technetium-99m Imaging Probe**

